Vibration and buckling of thin-walled composite I-beams with arbitrary lay-ups under axial loads and end moments

Thuc Phuong Vo* and Jaehong Lee†

Department of Architectural Engineering, Sejong University
98 Kunja Dong, Kwangjin Ku, Seoul 143-747, Korea

(Dated: April 21, 2011)

A finite element model with seven degrees of freedom per node is developed to study vibration and buckling of thin-walled composite I-beams with arbitrary lay-ups under constant axial loads and equal end moments. This model is based on the classical lamination theory, and accounts for all the structural coupling coming from material anisotropy. The governing differential equations are derived from the Hamilton's principle. Numerical results are obtained for thin-walled composite I-beams to investigate the effects of axial force, bending moment and fiber orientation on the buckling moments, natural frequencies and corresponding vibration mode shapes as well as axial-moment-frequency interaction curves.

Keywords: Thin-walled composite I-beams; fiber orientation; axial loads; end moments; axial-moment-frequency interaction curves

1. INTRODUCTION

Fiber-reinforced composite materials have been used over the past few decades in numerous types of structures. Composites have many desirable characteristics, such as high ratio of stiffness and strength to weight, corrosion resistance and magnetic transparency. Thin-walled structural shapes made up of composite materials, which are usually produced by pultrusion, are being increasingly used in many civil, mechanical and aerospace engineering applications. However, it is well known that thin-walled composite structures might be under axial force and moment simultaneously when used in above applications and are very susceptible to flexural-torsional/lateral buckling and display complex vibrational behavior. **Therefore, the behavior and accurate prediction of their stability and dynamic characteristics are of critical importance in the design of composite structures**.

The theory of thin-walled members made of isotropic materials was first developed by Vlasov [1] and Gjelsvik [2]. Since the early works of Bleich et al. [3] and Timoshenko et al. [4,5], **investigations into vibration and buckling**

*Present Address: Department of Engineering, University of Liverpool, Brownlow Street, Liverpool L69 3GQ, UK

†Professor, corresponding author. Tel.:+82-2-3408-3287; fax:+82-2-3408-3331

; Electronic address: jhlee@sejong.ac.kr

analyses of thin-walled beams subject simultaneously to axial loads and moments at both ends have been carried out extensively and only few are mentioned herein. Analytical solutions for the stability and vibrational behavior of thin-walled beams under combined loads have been performed by several authors. Joshi and Suryanarayan [6,7] derived solutions for coupled flexural-torsional vibration and instability. They found that the problem could be reduced to a beam-column problem with a zero moment, so that it was possible to obtain simple algebraic expressions unifying numerical results for various boundary conditions. Pavlovic et al. [8] obtained closed form analytical solutions for elastic stability problem of simply supported thin-walled beams subjected to time-dependent stochastic axial loads and end moments. Mohri et al [9] proposed analytical solutions for lateral buckling of simply supported bi-symmetric I-beams under combined bending and axial forces. Besides, the finite element method has been widely used because of its versatility and efficiency. Mohri et al. [10] presented a higher-order non shear deformable model to investigate the dynamic behavior of thin-walled open sections in the pre- and post-buckling state. Voros [11] analyzed the free vibration and mode shapes of straight beams where the coupling between the bending and torsion was induced by steady state lateral loads. As an alternative numerical method, the boundary element method [12-14] was developed to solve the vibration and buckling problems of the homogeneous or composite beams. The method overcomes the shortcoming of possible thin tube theory solution, which its utilization had been proven to be prohibitive even in thin-walled homogeneous sections. Another effective approach for solving stability and dynamic problems of thin-walled beams is to develop the dynamic stiffness matrix based on the solution of simultaneous ordinary differential equations. By using the power series method, Leung [15-18], developed the exact dynamic stiffness matrix including both the axial force, initial torque and bending moment for axial-lateral-torsional vibration, axial-torsional and axial-moment buckling analysis of framed structures. For thin-walled composite beams, with the presence of the additional coupling effects from material anisotropy, these members under axial force and moment simultaneously exhibit strong coupling. Therefore, their elastic stability behavior becomes more complicated than isotropic material even for doubly symmetric cross-section. **Although several authors have investigated the free vibration characteristics of axially loaded thin-walled composite beams (Bank and Kao [19], Banerjee et al. [20,21], Li et al. [22,23], Kaya and Ozgumus [24] and Kim et al. [25,26]), the existing literature reveals that studies of vibration and/or buckling of thin-walled composite beams under axial force and bending moment in a unitary manner are limited. Recently, Machado [27] derived analytical solutions for the lateral stability analysis of cross-ply laminated thin-walled beams subjected to combined axial and bending loads. Based on shear deformability, the theory was formulated in**

the context of large displacements and rotations, considering moderate bending rotations and large twist. However, composite was assumed to be made of symmetric balanced laminates and especially orthotropic laminates.

In previous works, Lee and Kim [28-30] focused separately the effect of axial loads on flexural-torsional buckling and bending loads on lateral buckling as well as free vibration of thin-walled composite I-beams with arbitrary lay-ups. This paper further investigates the effect of both axial loads and end moments on vibration and buckling of these beams. Axial-moment, load-frequency and axial-moment-frequency interaction curves with respect to the fiber angle change are presented. The duality among the buckling loads, buckling moments and natural frequencies is studied. This model is based on the classical lamination theory, and accounts for all the structural coupling coming from the material anisotropy. The governing differential equations for flexural-torsional coupled vibration and buckling are derived from the Hamilton's principle. A displacement-based one-dimensional finite element model with **seven degrees of freedom** per node is developed to solve the problem. Numerical results are obtained for thin-walled composite I-beams to investigate the effects of axial force, bending moment and fiber orientation on the buckling moments, natural frequencies and corresponding vibration mode shapes as well as interaction curves.

2. KINEMATICS

The theoretical developments presented in this paper require two sets of coordinate systems which are mutually interrelated. The first coordinate system is the orthogonal Cartesian coordinate system (x, y, z), for which the x and y axes lie in the plane of the cross section and the z axis parallel to the longitudinal axis of the beam. The second coordinate system is the local plate coordinate (n, s, z) as shown in Fig. 1, wherein the n axis is normal to the middle surface of a plate element, the s axis is tangent to the middle surface and is directed along the contour line of the cross section. The (n, s, z) and (x, y, z) coordinate systems are related through an angle of orientation θ. As defined in Fig. 1 a point P, called the pole, is placed at an arbitrary point x_p, y_p. A line through P parallel to the z axis is called the pole axis.

To derive the analytical model for **thin-walled open-section composite beams**, the following assumptions are made:

1. The contour of the thin wall does not deform in its own plane.

2. The linear shear strain $\bar{\gamma}_{sz}$ of the middle surface is zero in each element.

3. The Kirchhoff-Love assumption in classical plate theory remains valid for laminated composite thin-walled beams.

4. Each laminate is thin and perfectly bonded.

5. **Linear vibration and buckling analysis is examined**.

6. Local buckling is not considered.

According to assumption 1, the midsurface displacement components $\bar{u}, \bar{v}$ at a point A in the contour coordinate system can be expressed in terms of a displacements U, V of the pole P in the x, y directions, respectively, and the rotation angle Φ about the pole axis,

$$\bar{u}(s,z) = U(z)\sin\theta(s) - V(z)\cos\theta(s) - \Phi(z)q(s) \tag{1a}$$

$$\bar{v}(s,z) = U(z)\cos\theta(s) + V(z)\sin\theta(s) + \Phi(z)r(s) \tag{1b}$$

These equations apply to the whole contour. The out-of-plane shell displacement $\bar{w}$ can now be found from the assumption 2. For each element of middle surface, the shear strain become

$$\bar{\gamma}_{sz} = \frac{\partial \bar{v}}{\partial z} + \frac{\partial \bar{w}}{\partial s} = 0 \tag{2}$$

Eq.(2) can be integrated with respect to s from the origin to an arbitrary point on the contour,

$$\bar{w}(s,z) = W(z) - U'(z)x(s) - V'(z)y(s) - \Phi'(z)\omega(s) \tag{3}$$

where differentiation with respect to the axial coordinate z is denoted by primes ($'$); *W* **is an integration function that represents the average axial displacement of the beam in the z direction**; x and y are the coordinates of the contour in the (x, y, z) coordinate system; and ω is the so-called sectorial coordinate or warping function given by

$$\omega(s) = \int_{s_\circ}^{s} r(s)ds \tag{4}$$

The displacement components u, v, w representing the deformation of any generic point on the profile section are given with respect to the midsurface displacements $\bar{u}, \bar{v}, \bar{w}$ by the assumption 3.

$$u(s,z,n) = \bar{u}(s,z) \tag{5a}$$

$$v(s,z,n) = \bar{v}(s,z) - n\frac{\partial \bar{u}(s,z)}{\partial s} \tag{5b}$$

$$w(s,z,n) = \bar{w}(s,z) - n\frac{\partial \bar{u}(s,z)}{\partial z} \tag{5c}$$

The non-zero strains associated with the small-displacement theory of elasticity are given by

$$\epsilon_z = \frac{\partial w}{\partial z} = \bar{\epsilon}_z + n\bar{\kappa}_z \tag{6a}$$

$$\gamma_{sz} = \frac{\partial v}{\partial z} + \frac{\partial w}{\partial s} = n\bar{\kappa}_{sz} \tag{6b}$$

where

$$\bar{\epsilon}_z = \frac{\partial \bar{w}}{\partial z} = \epsilon_z^\circ + x\kappa_y + y\kappa_x + \omega\kappa_\omega \tag{7a}$$

$$\bar{\kappa}_z = -\frac{\partial^2 \bar{u}}{\partial z^2} = \kappa_y \sin\theta - \kappa_x \cos\theta - \kappa_\omega q \tag{7b}$$

$$\bar{\kappa}_{sz} = -2\frac{\partial^2 \bar{u}}{\partial s \partial z} = \kappa_{sz} \tag{7c}$$

The resulting strains can be obtained from Eqs.(6) and (7) as

$$\epsilon_z = \epsilon_z^\circ + (x + n\sin\theta)\kappa_y + (y - n\cos\theta)\kappa_x + (\omega - nq)\kappa_\omega \tag{8a}$$

$$\gamma_{sz} = n\kappa_{sz} \tag{8b}$$

where $\epsilon_z^\circ, \kappa_x, \kappa_y, \kappa_\omega$ and κ_{sz} are axial strain, biaxial curvatures in the x and y direction, warping curvature with respect to the shear center, and twisting curvature in the beam, respectively defined as

$$\epsilon_z^\circ = W' \tag{9a}$$

$$\kappa_x = -V'' \tag{9b}$$

$$\kappa_y = -U'' \tag{9c}$$

$$\kappa_\omega = -\Phi'' \tag{9d}$$

$$\kappa_{sz} = 2\Phi' \tag{9e}$$

3. VARIATIONAL FORMULATION

The total potential energy of the system can be stated as

$$\Pi = \mathcal{U} + \mathcal{V} \tag{10}$$

where $\mathcal{U}$ is the strain energy

$$\mathcal{U} = \frac{1}{2}\int_v (\sigma_z \epsilon_z + \sigma_{sz}\gamma_{sz}) dv \tag{11}$$

After substituting Eq.(8) into Eq.(11)

$$\mathcal{U} = \frac{1}{2}\int_v \left\{\sigma_z\Big[\epsilon_z^\circ + (x + n\sin\theta)\kappa_y + (y - n\cos\theta)\kappa_x + (\omega - nq)\kappa_\omega\Big] + \sigma_{sz}n\kappa_{sz}\right\}dv \tag{12}$$

The variation of strain energy can be stated as

$$\delta\mathcal{U} = \int_0^l (N_z\delta\epsilon_z + M_y\delta\kappa_y + M_x\delta\kappa_x + M_\omega\delta\kappa_\omega + M_t\delta\kappa_{sz})dz \tag{13}$$

where $N_z, M_x, M_y, M_\omega, M_t$ are axial force, bending moments in the x- and y-direction, warping moment (bimoment), and torsional moment, respectively, defined by integrating over the cross-sectional area A as

$$N_z = \int_A \sigma_z dsdn \tag{14a}$$
$$M_y = \int_A \sigma_z(x + n\sin\theta)dsdn \tag{14b}$$
$$M_x = \int_A \sigma_z(y - n\cos\theta)dsdn \tag{14c}$$
$$M_\omega = \int_A \sigma_z(\omega - nq)dsdn \tag{14d}$$
$$M_t = \int_A \sigma_{sz}ndsdn \tag{14e}$$

The potential of in-plane loads $\mathcal{V}$ due to transverse deflection

$$\mathcal{V} = \frac{1}{2}\int_v \overline{\sigma}_z^0\Big[(u')^2 + (v')^2\Big]dv \tag{15}$$

where $\overline{\sigma}_z^0$ is the averaged constant in-plane edge axial stress of beams loaded initially by equal and opposite axial forces P_0 and uniform bending moment applied about its major axis M_x^0 at two ends, defined by

$$\overline{\sigma}_z^0 = \frac{P_0}{A} - \frac{M_x^0 y}{I_x} \tag{16}$$

The variation of the potential of in-plane loads at the centroid is expressed by substituting the assumed displacement field into Eq.(15) as

$$\begin{aligned}\delta\mathcal{V} = \int_v (\frac{P_0}{A} - \frac{M_x^0 y}{I_x})\Big[&U'\delta U' + V'\delta V' + (q^2 + r^2 + 2rn + n^2)\Phi'\delta\Phi' \\ &+ (\Phi'\delta U' + U'\delta\Phi')\big[n\cos\theta - (y - y_p)\big] + (\Phi'\delta V' + V'\delta\Phi')\big[n\cos\theta + (x - x_p)\big]\Big]dv\end{aligned} \tag{17}$$

The kinetic energy of the system is given by

$$\mathcal{T} = \frac{1}{2}\int_v \rho(\dot{u}^2 + \dot{v}^2 + \dot{w}^2)dv \tag{18}$$

where ρ is a density.

The variation of the kinetic energy is expressed by substituting the assumed displacement field into Eq.(18) as

$$\begin{aligned}\delta\mathcal{T} &= \int_v \rho\Big\{\dot{U}\delta\dot{U} + \dot{V}\delta\dot{V} + \dot{W}\delta\dot{W} + (q^2+r^2+2rn+n^2)\dot{\Phi}\delta\dot{\Phi} + (\dot{\Phi}\delta\dot{U} + \dot{U}\delta\dot{\Phi})\Big[n\cos\theta - (y-y_p)\Big] \\ &+ (\dot{\Phi}\delta\dot{V} + \dot{V}\delta\dot{\Phi})\Big[n\cos\theta + (x-x_p)\Big]\Big\}dv \end{aligned} \tag{19}$$

In order to derive the equations of motion, Hamilton's principle is used

$$\delta\int_{t_1}^{t_2}(\mathcal{T}-\Pi)dt \;=\; 0 \tag{20}$$

Substituting Eqs.(13),(17) and (19) into Eq.(20), the following weak statement is obtained

$$\begin{aligned} 0 &= \int_{t_1}^{t_2}\int_0^l \Big\{m_0\dot{W}\delta\dot{W} + \Big[m_0\dot{U} + (m_c+m_0y_p)\dot{\Phi}\Big]\delta\dot{U} + \Big[m_0\dot{V} + (m_s-m_0x_p)\dot{\Phi}\Big]\delta\dot{V} \\ &+ \Big[(m_c+m_0y_p)\dot{U} + (m_s-m_0x_p)\dot{V} + (m_p+m_2+2m_\omega)\dot{\Phi}\Big]\delta\dot{\Phi} \\ &- \Big[P_0\big[\delta U'(U'+\Phi'y_p) + \delta V'(V'-\Phi'x_p) + \delta\Phi'(\Phi'\frac{I_p}{A} + U'y_p - V'x_p)\big] - M_x^0(\Phi\delta U'' + U''\delta\Phi)\Big] \\ &- N_z\delta W' + M_y\delta U'' + M_x\delta V'' + M_\omega\delta\Phi'' - 2M_t\delta\Phi\Big\}dzdt \end{aligned} \tag{21}$$

The expressions of inertia coefficients for thin-walled composite beams are given in Ref. [30].

4. CONSTITUTIVE EQUATIONS

The constitutive equations of a k^{th} orthotropic lamina in the laminate co-ordinate system of section are given by

$$\begin{Bmatrix}\sigma_z\\ \sigma_{sz}\end{Bmatrix}^k = \begin{bmatrix}\bar{Q}_{11}^* & \bar{Q}_{16}^*\\ \bar{Q}_{16}^* & \bar{Q}_{66}^*\end{bmatrix}^k \begin{Bmatrix}\epsilon_z\\ \gamma_{sz}\end{Bmatrix} \tag{22}$$

where $\bar{Q}_{ij}^*$ are transformed reduced stiffnesses. The transformed reduced stiffnesses can be calculated from the transformed stiffnesses based on the plane stress ($\sigma_s = 0$) and plane strain ($\epsilon_s = 0$) assumption. More detailed explanation can be found in Ref. [31].

The constitutive equations for bar forces and bar strains are obtained by using Eqs.(8), (14) and (22)

$$\begin{Bmatrix}N_z\\ M_y\\ M_x\\ M_\omega\\ M_t\end{Bmatrix} = \begin{bmatrix} E_{11} & E_{12} & E_{13} & E_{14} & E_{15}\\ & E_{22} & E_{23} & E_{24} & E_{25}\\ & & E_{33} & E_{34} & E_{35}\\ & & & E_{44} & E_{45}\\ \text{sym.} & & & & E_{55}\end{bmatrix} \begin{Bmatrix}\epsilon_z^\circ\\ \kappa_y\\ \kappa_x\\ \kappa_\omega\\ \kappa_{sz}\end{Bmatrix} \tag{23}$$

where E_{ij} are stiffnesses of thin-walled composite beams and given in Ref. [30].

5. GOVERNING EQUATIONS OF MOTION

The governing equations of motion of the present study can be derived by integrating the derivatives of the varied quantities by parts and collecting the coefficients of of $\delta W, \delta U, \delta V$ and $\delta\Phi$

$$N_z' = m_0\ddot{W} \tag{24a}$$

$$M_y'' + P_0\big(U'' + \Phi'' y_p\big) + M_x^0\Phi'' = m_0\ddot{U} + (m_c + m_0 y_p)\ddot{\Phi} \tag{24b}$$

$$M_x'' + P_0\big(V'' - \Phi'' x_p\big) = m_0\ddot{V} + (m_s - m_0 x_p)\ddot{\Phi} \tag{24c}$$

$$\begin{aligned} M_\omega'' + 2M_t' + P_0\big(\Phi''\frac{I_p}{A} + U'' y_p - V'' x_p\big) + M_x^0 U'' &= (m_c + m_0 y_p)\ddot{U} \\ &+ (m_s - m_0 x_p)\ddot{V} \\ &+ (m_p + m_2 + 2m_\omega)\ddot{\Phi} \end{aligned} \tag{24d}$$

The natural boundary conditions are of the form

$$\delta W \ : \ N_z = P_0 \tag{25a}$$

$$\delta U \ : \ M_y' = {M_y'}^0 \tag{25b}$$

$$\delta U' \ : \ M_y = M_y^0 \tag{25c}$$

$$\delta V \ : \ M_x' = {M_x'}^0 \tag{25d}$$

$$\delta V' \ : \ M_x = M_x^0 \tag{25e}$$

$$\delta\Phi \ : \ M_\omega' + 2M_t = {M_\omega'}^0 \tag{25f}$$

$$\delta\Phi' \ : \ M_\omega = M_\omega^0 \tag{25g}$$

where $P_0, {M_y'}^0, M_y^0, {M_x'}^0, M_x^0, {M_\omega'}^0$ and M_ω^0 are prescribed values.

By substituting Eqs.(9) and (23) into Eq.(24), the explicit form of governing equations of motion can be expressed

with respect to the laminate stiffnesses E_{ij} as

$$E_{11}W'' - E_{12}U''' - E_{13}V''' - E_{14}\Phi''' + 2E_{15}\Phi'' = m_0\ddot{W} \tag{26a}$$

$$E_{12}W''' - E_{22}U^{iv} - E_{23}V^{iv} - E_{24}\Phi^{iv} + 2E_{25}\Phi''' + P_0(U'' + \Phi'' y_p) + M_x^0\Phi'' = m_0\ddot{U} + (m_c + m_0 y_p)\ddot{\Phi} \tag{26b}$$

$$E_{13}W''' - E_{23}U^{iv} - E_{33}V^{iv} - E_{34}\Phi^{iv} + 2E_{35}\Phi''' + P_0(V'' - \Phi'' x_p) = m_0\ddot{V} + (m_s - m_0 x_p)\ddot{\Phi} \tag{26c}$$

$$\begin{aligned} E_{14}W''' + 2E_{15}W'' - E_{24}U^{iv} - 2E_{25}U''' - E_{34}V^{iv} - 2E_{35}V''' \\ -E_{44}\Phi^{iv} + 4E_{55}\Phi'' + P_0(\Phi''\frac{I_p}{A} + U'' y_p - V'' x_p) + M_x^0 U'' &= (m_c + m_0 y_p)\ddot{U} \\ &+ (m_s - m_0 x_p)\ddot{V} \\ &+ (m_p + m_2 + 2m_\omega)\ddot{\Phi} \end{aligned} \tag{26d}$$

Eq.(26) is most general form for elastic stability of thin-walled composite beams with arbitrary lay-ups under constant axial loads and equal end moments and the dependent variables, W, U, V and Φ are fully coupled. If all the **coupling effects are neglected** and the cross section is symmetrical with respect to both x- and the y-axes, Eq.(26) can be simplified to the uncoupled differential equations as

$$(EA)_{com}W'' = \rho A\ddot{W} \tag{27a}$$

$$-(EI_y)_{com}U^{iv} + P_0U'' + M_x^0\Phi'' = \rho A\ddot{U} \tag{27b}$$

$$-(EI_x)_{com}V^{iv} + P_0V'' = \rho A\ddot{V} \tag{27c}$$

$$-(EI_\omega)_{com}\Phi^{iv} + \Big[(GJ)_{com} + P_0\frac{I_p}{A}\Big]\Phi'' + M_x^0U'' = \rho I_p\ddot{\Phi} \tag{27d}$$

From above equations, $(EA)_{com}$ represents axial rigidity, $(EI_x)_{com}$ and $(EI_y)_{com}$ represent flexural rigidities with respect to x- and y-axis, $(EI_\omega)_{com}$ represents warping rigidity, and $(GJ)_{com}$ represents torsional rigidity of thin-walled composite beams, respectively, written as

$$(EA)_{com} = E_{11} \tag{28a}$$

$$(EI_y)_{com} = E_{22} \tag{28b}$$

$$(EI_x)_{com} = E_{33} \tag{28c}$$

$$(EI_\omega)_{com} = E_{44} \tag{28d}$$

$$(GJ)_{com} = 4E_{55} \tag{28e}$$

A. Flexural-torsional vibration under axial loads and equal end moments

For simply supported beams with free warping, the overall displacements modes in bending and torsion are assumed as

$$U(z,t) = U_0 \sin(\frac{n\pi z}{L}) \sin(\omega t) \tag{29a}$$

$$V(z,t) = V_0 \sin(\frac{n\pi z}{L}) \sin(\omega t) \tag{29b}$$

$$\Phi(z,t) = \Phi_0 \sin(\frac{n\pi z}{L}) \sin(\omega t) \tag{29c}$$

Substituting Eq.(29) into Eq.(27), after integrations and some reductions, the resulting flexural and torsional equations of motion are obtained in compact form as

$$\omega_{x_n}^2 (1 - \overline{P}_{x_n}) - \omega_{xx_n}^2 = 0 \tag{30a}$$

$$A\Big[\omega_{y_n}^2 (1 - \overline{P}_{y_n}) - \omega^2\Big] U_0 - \overline{M}_{x_n} \sqrt{AI_p} \omega_{y_n} \omega_{\theta_n} \Phi_0 = 0 \tag{30b}$$

$$-\overline{M}_{x_n} \sqrt{AI_p} \omega_{y_n} \omega_{\theta_n} U_0 + I_p \Big[\omega_{\theta_n}^2 (1 - \overline{P}_{\theta_n}) - \omega^2\Big] \Phi_0 = 0 \tag{30c}$$

The flexural natural frequencies in the x-direction and bending moments are decoupled, while, the flexural natural frequencies in the y-direction, torsional natural frequencies and bending moments are coupled.

$$\omega_{xx_n} = \omega_{x_n} \sqrt{1 - \overline{P}_{x_n}} \tag{31a}$$

$$\omega_{ya_n} = \sqrt{\frac{\omega_{y_n}^2 (1 - \overline{P}_{y_n}) + \omega_{\theta_n}^2 (1 - \overline{P}_{\theta_n})}{2} - \sqrt{\Big[\frac{\omega_{y_n}^2 (1 - \overline{P}_{y_n}) - \omega_{\theta_n}^2 (1 - \overline{P}_{\theta_n})}{2}\Big]^2 + \overline{M}_n^2 \omega_{y_n}^2 \omega_{\theta_n}^2}} \tag{31b}$$

$$\omega_{yb_n} = \sqrt{\frac{\omega_{y_n}^2 (1 - \overline{P}_{y_n}) + \omega_{\theta_n}^2 (1 - \overline{P}_{\theta_n})}{2} + \sqrt{\Big[\frac{\omega_{y_n}^2 (1 - \overline{P}_{y_n}) - \omega_{\theta_n}^2 (1 - \overline{P}_{\theta_n})}{2}\Big]^2 + \overline{M}_n^2 \omega_{y_n}^2 \omega_{\theta_n}^2}} \tag{31c}$$

in which $\overline{P}_{x_n}, \overline{P}_{y_n}, \overline{P}_{\theta_n}$ and $\overline{M}_{x_n}$ are nondimensional axial force and moment parameters

$$\overline{P}_{x_n} = \frac{P_0}{P_{x_n}} \tag{32a}$$

$$\overline{P}_{y_n} = \frac{P_0}{P_{y_n}} \tag{32b}$$

$$\overline{P}_{\theta_n} = \frac{P_0}{P_{\theta_n}} \tag{32c}$$

$$\overline{M}_{x_n} = \frac{M_x^0}{M_{y\theta_n}} \tag{32d}$$

where P_{x_n}, P_{y_n} and P_{θ_n} are the flexural buckling loads in the x- and y-direction, and torsional buckling loads [4].

$$P_{x_n} = \frac{n^2\pi^2(EI_x)_{com}}{l^2} \tag{33a}$$

$$P_{y_n} = \frac{n^2\pi^2(EI_y)_{com}}{l^2} \tag{33b}$$

$$P_{\theta_n} = \frac{A}{I_p}\Big[\frac{n^2\pi^2(EI_\omega)_{com}}{l^2} + (GJ)_{com}\Big] \tag{33c}$$

and $M_{y\theta_n}$ is the buckling moments for pure bending [4].

$$M_{y\theta_n} = \sqrt{\frac{n^2\pi^2(EI_y)_{com}}{l^2}\Big[\frac{n^2\pi^2(EI_\omega)_{com}}{l^2} + (GJ)_{com}\Big]} \tag{34}$$

and $\omega_{x_n}, \omega_{y_n}$ and ω_{θ_n} are the flexural natural frequencies in the x- and y-direction, and torsional natural frequencies [5].

$$\omega_{x_n} = \frac{n^2\pi^2}{l^2}\sqrt{\frac{(EI_x)_{com}}{\rho A}} \tag{35a}$$

$$\omega_{y_n} = \frac{n^2\pi^2}{l^2}\sqrt{\frac{(EI_y)_{com}}{\rho A}} \tag{35b}$$

$$\omega_{\theta_n} = \frac{n\pi}{l}\sqrt{\frac{1}{\rho I_p}\Big[\frac{n^2\pi^2}{l^2}(EI_\omega)_{com} + (GJ)_{com}\Big]} \tag{35c}$$

B. Flexural-torsional buckling under axial loads and equal end moments

By omitting the inertia terms, Eq.(27) becomes

$$(EA)_{com}W'' = 0 \tag{36a}$$

$$-(EI_y)_{com}U^{iv} + P_0U'' + M_x^0\Phi'' = 0 \tag{36b}$$

$$-(EI_x)_{com}V^{iv} + P_0V'' = 0 \tag{36c}$$

$$-(EI_\omega)_{com}\Phi^{iv} + \Big[(GJ)_{com} + P_0\frac{I_p}{A}\Big]\Phi'' + M_x^0U''' = 0 \tag{36d}$$

It is well known that the flexural buckling loads in the x-direction are identified while the flexural buckling loads in the y-direction, torsional buckling loads and buckling moments are coupled. The orthotropy solution for the critical values of axial force P_0 and bending moment M_x^0 [4]

$$M_x^0 = r_p\sqrt{P_\theta P_y(1-\frac{P_0}{P_y})(1-\frac{P_0}{P_\theta})} \tag{37}$$

where P_x, P_y and P_θ are the critical flexural buckling load in the x- and y-direction, and the critical torsional buckling load, can be obtained from Eq.(33).

6. FINITE ELEMENT FORMULATION

The present theory for thin-walled composite beams described in the previous section was implemented via a displacement based finite element method. The element has seven degrees of freedom at each node, three displacements W, U, V and three rotations U', V', Φ as well as one warping degree of freedom Φ'. The axial displacement W is interpolated using linear shape functions $\hat{\psi}_j$, whereas the lateral and vertical displacements U, V and axial rotation Φ are interpolated using Hermite-cubic shape functions ψ_j associated with node j and the nodal values, respectively.

$$W = \sum_{j=1}^{2} w_j \hat{\psi}_j \tag{38a}$$

$$U = \sum_{j=1}^{4} u_j \psi_j \tag{38b}$$

$$V = \sum_{j=1}^{4} v_j \psi_j \tag{38c}$$

$$\Phi = \sum_{j=1}^{4} \phi_j \psi_j \tag{38d}$$

Substituting these expressions into the weak statement in Eq.(21), the finite element model of a typical element can be expressed as the standard eigenvalue problem

$$([K] - P_0[G_1] - M_x^0[G_2] - \omega^2[M])\{\Delta\} = \{0\} \tag{39}$$

where $[K], [G_1], [G_2]$ and $[M]$ are the element stiffness matrix, the element geometric stiffness matrix due to axial force, bending moment and the element mass matrix, respectively. The explicit forms of them are given in Refs. [28-30].

In Eq.(39), $\{\Delta\}$ is the eigenvector of nodal displacements corresponding to an eigenvalue

$$\{\Delta\} = \{W\ U\ V\ \Phi\}^{\mathrm{T}} \tag{40}$$

7. NUMERICAL EXAMPLES

For verification purpose, the buckling behavior and free vibration of a cantilever symmetrically laminated mono-symmetric I-beam with length $l = 1$m under axial load at the centroid is performed. Following dimensions for the I-beam are used: the height, top and bottom flange widths are 50mm, 30mm and 50mm, respectively. The flanges and web are made of sixteen layers with each layer 0.13mm in thickness. All computations are carried out for the glass-epoxy materials with the following material properties: $E_1 = 53.78$GPa , $E_2 = 17.93$GPa , $G_{12} = 8.96$GPa , $\nu_{12} =$

$0.25, \rho = 1968.9\text{kg/m}^3$. The critical buckling loads are evaluated and compared with numerical results of Kim and Shin [26], which is based on dynamic stiffness formulation and ABAQUS solutions in Table 1. Next, the flexural-torsional coupled vibration analysis of axially loaded cantilever beam is analyzed. The applied magnitude of axial force is given in Ref. [26], which corresponds to one half of buckling load of beam. The lowest four coupled natural frequencies with and without the axial force are presented in Table 2. Load-frequency interaction curves for fiber angles 0°, 30° and 60° is exhibited in Fig. 2. It reveals that the tension force has a stiffening effect while the compressive force has a softening effect on the natural frequencies. **The accuracy of the prediction from present model with Kim and Shin [26] can be seen in Tables 1 and 2, except for some natural frequencies in higher modes. However, maximum difference is small, nearly 2.5% and within the acceptable range**.

To illustrate the accuracy of this study further, a simply supported composite doubly symmetric I-beam with length $l = 5.0$m under an eccentric load is analyzed. Lay-ups and material properties are the same with previous example except the geometry of I-section. Both of flanges width b and web height h are 50mm. The critical buckling loads of this beam under an axial compressive force acting at positions of $e = 0, h/4$ and $h/2$ from the centroid are calculated. The comparison of the results between the proposed finite element analysis and analytical approach by Kim et al. [32] is given in Table 3. The present solution again indicates good agreement with the analytical solution and ABAQUS results for all lamination schemes considered. Next, besides the eccentric load, this simply supported beam under an additional uniform bending moment simultaneously is performed to study effect of eccentricity on the buckling moments. The axial-moment interaction curves for various fiber angles are plotted in Fig. 3. The critical buckling moments for pure bending occur at about M=42.28Nm, 62.47Nm and 65.13Nm for fiber angles 60°, 30° and 0°, respectively. It is clear that with the presence of the axial compressive force, the eccentricity decreases both buckling loads and moments. The relative difference of these results due to the eccentricity is significant and maximum at unidirectional fiber angle (Fig. 3 and Table 3).

In order to investigate the effect of axial force, bending moment, fiber orientation on the buckling moments, natural frequencies and corresponding vibration mode shapes as well as axial-moment-frequency interaction curves, a simply supported composite I-beam with length $l = 8$m under axial force and uniform bending moment is considered. The geometry and stacking sequences of this simply supported beam are shown in Fig. 4, and the following engineering constants are used

$$E_1/E_2 = 25, G_{12}/E_2 = 0.6, \nu_{12} = 0.25 \tag{41}$$

For convenience, the following nondimensional axial force, bending moment and natural frequency are used

$$\overline{P} = \frac{P_0 l^2}{b_3^3 t E_2} \tag{42a}$$

$$\overline{M} = \frac{M_x^0 l}{b_3^3 t E_2} \tag{42b}$$

$$\overline{\omega} = \frac{\omega l^2}{b_3}\sqrt{\frac{\rho}{E_2}} \tag{42c}$$

Stacking sequences of the flanges and web are angle-ply laminates $[\theta/-\theta]$, (Fig. 4a). All the coupling stiffnesses are zero, but E_{15}, E_{35} do not vanish due to unsymmetric lay-up of the flanges and web. Effect of axial force on the critical buckling moments ($\overline{M}_{cr}$) is shown in Table 4. The critical buckling loads and the critical buckling moments without axial force agree completely with those of previous papers [28,29]. In Table 5, with the presence of bending moment, the lowest four natural frequencies with and without the effect of axial force by the finite element analysis are compared to those of the orthotropy solution, which neglects the coupling effects of E_{15}, E_{35} from Eqs.(31a)-(31c). It can be seen that the change in the critical buckling moments and natural frequencies due to axial force is noticeable for all fiber angles. The results diminish when the axial force changes from tensile to compressive, as expected. This demonstrates again the fact that a tensile force stiffens the beam and a compressive force softens the beam. For unidirectional fiber direction, the results by the finite element analysis exactly correspond to those by the orthotropy solution (Tables 4 and 5). At this fiber angle, the lowest four natural frequencies are the first, second and third flexural-torsional coupled modes and the first flexural mode in x-direction, respectively. As fiber angle changes, **this order changes a bit**. It can be explained by the typical normal mode shapes corresponding to the lowest four natural frequencies with fiber angle $\theta = 30^\circ$ for the case ($\overline{P} = 0.5\overline{P}_{cr}$, $\overline{M} = 0.5\overline{M}_{cr}$) in Fig. 5. Relative measures of flexural displacements, torsional rotation show that when the beam is vibrating at the natural frequency belonging to the first and second mode exhibits doubly coupled vibrations (flexural mode in y-direction and torsional mode), whereas, third and fourth mode display triply coupled vibrations (flexural mode in the x-, y-direction and torsional mode). Due to the small coupling stiffnesses E_{15}, E_{35}, the results by the finite element analysis and orthotropy solution show slight discrepancy in the range $\theta \in [15^\circ - 60^\circ]$. However, as fiber angle increases, the coupling effects from material anisotropy become negligible. Therefore, the orthotropy solution and the finite element analysis are nearly identical. In order to investigate the effects of bending moment on the critical buckling loads and natural frequencies, the axial-moment and moment-frequency interaction curves for the fiber angles $\theta = 30^\circ$ and 60° of two solutions are plotted in Figs. 6-8. All of the interaction curves are symmetric with respect to the $\overline{M} = 0$ axis. **The moment at buckling increase from zero as the axial compressive force decreases from the buckling**

load to the buckling moment when $\overline{P} = 0$, as shown in Fig. 6. Further increases take place after axial force becomes negative (tensile). Characteristic of axial-moment and moment-frequency interaction curves is that the value of the bending moment for which the axial force or natural frequency vanishes constitutes the buckling moment. For example, for $\theta = 30^\circ$ (Fig. 7), when the beam is under an axial compressive force ($\overline{P} = 0.5\overline{P}_{cr}$), the first buckling moment occurs at $\overline{M} = 2.36 \times 10^{-2}$, which agrees completely with value from Table 4. As a result, the lowest branch is disappeared when $\overline{M}$ is slightly over this value. As the bending moment increases, two interaction curves ($\omega_2 - M_2$) and ($\omega_3 - M_3$) intersect at $\overline{M} = 5.37 \times 10^{-2}$, thus, after this value, vibration mode 2 and 3 change each other. The second branch will also be disappeared when $\overline{M}$ is slightly over 8.44×10^{-2}, which is corresponding to the second buckling moment. Fig. 9 shows a comprehensive three dimensional axial-moment-frequency interaction diagram. Two groups of curves are observed. The small group is for $\theta = 60^\circ$ and the larger group is for $\theta = 45^\circ$. It is clear that moment-frequency interaction curves become smaller as the axial compressive force increases. Finally, these curves vanish at about $\overline{P} = 0.25$ and 0.45 for fiber angle $\theta = 60^\circ$ and 45°, respectively, which implies that at these loads, the critical bucklings occur as a degenerated case of natural vibration at zero frequency and bending moment at zero value.

The next example is the same as before except that in this case, the bottom flange is angle-ply laminates $[\theta/-\theta]$, while the top flange and web laminates are unidirectional, (Fig. 4b). Major effects of axial force and bending moment on the critical buckling moments and natural frequencies are again seen Tables 6 and 7. As the fiber angle changes, the orthotropy solution and the finite element analysis solution show discrepancy indicating the coupling effects become significant. That is, the orthotropy solution is no longer valid for unsymmetrically laminated beams, and triply flexural-torsional coupled vibration and buckling should be considered even for bisymmetric thin-walled composite beams. The effect of axial force on the critical buckling moments with the fiber angles 30° and 60° is plotted in Fig. 10. When the axial force is compressive, this beam has two different critical buckling moments. The higher one of these is positive and occurs when the moment causes compression in the top flange, while the lower one is negative, corresponding to a reversal in the sense of the moment which causes tension in the top flange. On the other hand, when the axial force is tensile, the higher buckling moment is negative and lower one is positive. Beside, it tends to stabilize the beam, and the critical buckling moments are increased, as expected. The lowest three moment-frequency interaction curves with the fiber angle $\theta = 60^\circ$ for two cases ($\overline{P} = -0.5\overline{P}_{cr}$) and ($\overline{P} = 0.5\overline{P}_{cr}$) are displayed in Figs. 11 and 12. With the increase of bending moment, after the first and third natural frequencies increase and reach local maximum values, they decrease. The increase and decrease become steeper when bending moments are close

to buckling moments. It is from Figs. 10-12 that highlights the effects of coupling on the vibration and buckling of thin-walled composite beam under constant axial loads and equal end moments. All of the symmetric axial-moment and moment-frequency interaction curves are no longer visible. This response is never seen in bisymmetric thin-walled isotropic beams because the coupling terms are not present. It is similar to the behavior of monosymmetric beams, which implies that due to coupling effects when thin-walled composite beams under axial force and bending moment, for each value of axial force or natural frequency always corresponding to two unequal values of buckling moment. Figs. 10-12 also explain the duality among buckling moment, critical buckling load and natural frequency.

8. CONCLUDING REMARKS

Vibration and buckling of **thin-walled composite I-beams** with arbitrary lay-ups under axial loads and end moments is presented. This model is capable of predicting accurately the buckling moments, natural frequencies and corresponding vibration mode shapes as well as axial-moment-frequency interaction curves. To formulate the problem, a one-dimensional displacement-based finite element method with **seven degrees of freedom** per node is developed. All of the possible vibration mode shapes including the flexural mode in the x- and y-direction and the torsional mode, and fully flexural-torsional coupled mode are included in the analysis. The present model is found to be appropriate and efficient in analyzing vibration and buckling problem of **thin-walled composite I-beams** under constant axial loads and equal end moments.

Acknowledgments

This research was supported by Basic Research Laboratory Program of the National Research Foundation of Korea (NRF) funded by the Ministry of Education, Science and Technology through NRF2010-0019373, and by Korea Ministry of Knowledge Economy under the national HRD support program for convergence information technology supervised by National IT Industry Promotion Agency through NIPA-2010-C6150-1001-0013.

References

[1] V. Z. Vlasov, Thin Walled Elastic Beams, Israel Program for Scientific Transactions, Jerusalem, 1961.

[2] A. Gjelsvik, The theory of thin walled bars, Wiley, New York, 1981.

[3] F. Bleich, L. Ramsey, H. Bleich, Buckling strength of metal structures, McGraw-Hill, New York, 1952.

[4] S. Timoshenko, J. M. Gere, Theory of elastic stability, McGraw-Hill, New York, 1961.

[5] S. Timoshenko, D. H. Young, W. J. R. Weaver, Vibration problems in engineering, John Wiley & Sons, New York, 1974.

[6] A. Joshi, S. Suryanarayan, A unified solution for various boundary conditions for the coupled flexural-torsional instability of closed thin-walled beam-columns, Int J Solids Struct 20 (2) (1984) 167 – 178.

[7] A. Joshi, S. Suryanarayan, Unified analytical solution for various boundary conditions for the coupled flexural-torsional vibration of beams subjected to axial loads and end moments, J Sound Vib 129 (2) (1989) 313 – 326.

[8] R. Pavlovic, P. Kozic, P. Rajkovic, I. Pavlovic, Dynamic stability of a thin-walled beam subjected to axial loads and end moments, J Sound Vib 301 (3-5) (2007) 690 – 700.

[9] F. Mohri, C. Bouzerira, M. Potier-Ferry, Lateral buckling of thin-walled beam-column elements under combined axial and bending loads, Thin-Walled Struct 46 (3) (2008) 290 – 302.

[10] F. Mohri, L. Azrar, M. Potier-Ferry, Vibration analysis of buckled thin-walled beams with open sections, J Sound Vib 275 (1-2) (2004) 434 – 446.

[11] G. M. Voros, On coupled bending-torsional vibrations of beams with initial loads, Mech Res Commun 36 (5) (2009) 603 – 611.

[12] E. J. Sapountzakis, G. C. Tsiatas, Flexural-torsional Vibrations of Beams by BEM, Comput Mech 39 (4) (2007) 409–417.

[13] E. J. Sapountzakis, G. C. Tsiatas, Flexural - torsional buckling and vibration analysis of composite beams, Comput Mater Con 6(2) (2007) 103–115.

[14] E. J. Sapountzakis, J. Dourakopoulos, Lateral buckling analysis of beams of arbitrary cross section by BEM, Comput Mech 45 (1) (2009) 11–21.

[15] A. Y. T. Leung, Dynamic stiffness analysis for axial-lateral-torsional vibration, Dynamical Systems: An International Journal 8 (1) (1993) 19 – 30.

[16] A. Y. T. Leung, Exact dynamic stiffness for axial-torsional buckling of structural frames, Thin-Walled Struct 46 (1) (2008) 1 – 10.

[17] A. Y. T. Leung, Dynamic axial-moment buckling of linear beam systems by power series stiffness, J Eng Mech 135 (8) (2009) 852–861.

[18] A. Y. T. Leung, Nonconservative dynamic axial-torsional buckling of structural frames using power series, Int J Mech Sci In 51 (11-12) (2009) 807–815.

[19] L. C. Bank, C. Kao, Dynamic Response of Thin-Walled Composite Material Timoshenko Beams, J Energ Resour 112 (2) (1990) 149–154.

[20] J. R. Banerjee, F. W. Williams, Exact dynamic stiffness matrix for composite Timoshenko beams with applications, J Sound Vib 194 (4) (1996) 573 – 585.

[21] J. R. Banerjee, Free vibration of axially loaded composite Timoshenko beams using the dynamic stiffness matrix method, Comput Struct 69 (2) (1998) 197 – 208.

[22] J. Li, R. Shen, H. Hua, J. Xianding, Bending-torsional coupled dynamic response of axially loaded composite Timosenko thin-walled beam with closed cross-section, Compos Struct 64 (1) (2004) 23 – 35.

[23] J. Li, G. Wu, R. Shen, H. Hua, Stochastic bending-torsion coupled response of axially loaded slender composite-thin-walled beams with closed cross-sections, Int J Mech Sci 47 (1) (2005) 134 – 155.

[24] M. Kaya, O. O. Ozgumus, Flexural-torsional-coupled vibration analysis of axially loaded closed-section composite Timoshenko beam by using DTM, J Sound Vib 306 (3-5) (2007) 495 – 506.

[25] N. I. Kim, D. K. Shin, Y. S. Park, Dynamic stiffness matrix of thin-walled composite I-beam with symmetric and arbitrary laminations, J Sound Vib 318 (1-2) (2008) 364 – 388.

[26] N. I. Kim, D. K. Shin, Dynamic stiffness matrix for flexural-torsional, lateral buckling and free vibration analyses of mono-symmetric thin-walled composite beams, Int J Struct Stab Dy 9 (3) (2009) 411–436.

[27] Machado, S. P. Interaction of combined loads on the lateral stability of thin-walled composite beams Eng Struct 32 (11) (2010) 3516–3527

[28] J. Lee, S. E. Kim, Flexural-torsional buckling of thin-walled I-section composites, Comput Struct 79 (10) (2001) 987 – 995.

[29] J. Lee, S. E. Kim, K. Hong, Lateral buckling of I-section composite beams, Eng Struct 24 (7) (2002) 955 – 964.

[30] J. Lee, S. E. Kim, Free vibration of thin-walled composite beams with I-shaped cross-sections, Compos Struct 55 (2) (2002) 205 – 215.

[31] R. M. Jones, Mechanics of Composite Materials, Taylor & Francis, 1999.

[32] N. I. Kim, D. K. Shin, M. Y. Kim, Improved flexural-torsional stability analysis of thin-walled composite beam and exact stiffness matrix, Int J Mech Sci 49 (8) (2007) 950 – 969.

CAPTIONS OF TABLES

Table 1: Critical bucking loads (N) of a cantilever mono-symmetric composite I-beam with symmetric angle-ply laminates $[\pm\theta]_{4s}$ in the flanges and web.

Table 2: Natural frequencies (Hz) of a cantilever mono-symmetric composite I-beam with symmetric angle-ply laminates $[\pm\theta]_{4s}$ in the flanges and web under constant axial forces at the centroid (( ): natural frequency with an axial compressive force, [ ]: natural frequency with an axial tensile force).

Table 3: Effect of eccentricity on critical bucking loads (N) of a simply supported composite I-beam with symmetric angle-ply laminates $[\pm\theta]_{4s}$ in the flanges and web.

Table 4: Effect of axial force on the critical buckling moments $\overline{M}_{cr}(\times 10^{-2})$ of a simply supported composite beam with respect to the fiber angle change in the flanges and web.

Table 5: Effect of axial force and bending moment on the first four natural frequencies of a simply supported composite beam with respect to the fiber angle change in the flanges and web.

Table 6: Effect of axial force on the critical buckling moments $\overline{M}_{cr}(\times 10^{-2})$ of a simply supported composite beam with respect to the fiber angle change in the bottom flange.

Table 7: Effect of axial force and bending moment on the first four natural frequencies of a simply supported composite beam with respect to the fiber angle change in the bottom flange.

CAPTIONS OF FIGURES

Figure 1: Definition of coordinates in thin-walled open-section composite beams.

Figure 2: Effect of axial force on the fundamental natural frequency with the fiber angles 0°, 30° and 60° in the flanges and web of a cantilever mono-symmetric composite I-beam.

Figure 3: Effect of eccentricity and axial compressive force on the critical buckling moments with the fiber angles 0°, 30° and 60° in the flanges and web of a simply supported composite beam.

Figure 4: Geometry and stacking sequences of a simply supported I-beam under axial load and uniform bending.

Figure 5: The first four normal mode shapes of the flexural and torsional components with the fiber angle 30° in the flanges and web of a simply supported composite beam under an axial compressive force ($\overline{P} = 0.5\overline{P}_{cr}$) and bending moment ($\overline{M} = 0.5\overline{M}_{cr}$).

Figure 6: Effect of axial force on the critical buckling moments with the fiber angles 30° and 60° in the flanges and web of a simply supported composite beam.

Figure 7: Effect of bending moment on the first three natural frequencies with the fiber angle 30° in the bottom flange of a simply supported composite beam under an axial compressive force ($\overline{P} = 0.5\overline{P}_{cr}$).

Figure 8: Effect of bending moment on the first three natural frequencies with the fiber angle 60° in the bottom flange of a simply supported composite beam under an axial compressive force ($\overline{P} = 0.5\overline{P}_{cr}$).

Figure 9: Three dimensional interaction diagram of the fundamental natural frequency, bending moment and axial compressive force with the fiber angle 45° and 60° in the flanges and web of a simply supported composite beam.

Figure 10: Effect of axial force on the critical buckling moments with the fiber angles 30° and 60° in the bottom flange of a simply supported composite beam.

Figure 11: Effect of bending moment on the first three natural frequencies with the fiber angle 60° in the bottom flange of a simply supported composite beam under an axial tensile force ($\overline{P} = -0.5\overline{P}_{cr}$).

Figure 12: Effect of bending moment on the first three natural frequencies with the fiber angle 60° in the bottom flange of a simply supported composite beam under an axial compressive force ($\overline{P} = 0.5\overline{P}_{cr}$).

TABLE 1 Critical bucking loads (N) of a cantilever mono-symmetric composite I-beam with symmetric angle-ply laminates $[\pm\theta]_{4s}$ in the flanges and web.

Lay-ups	Kim and Shin [26]		Present
	ABAQUS	No shear	
$[0]_{16}$	2969.7	2998.1	2998.2
$[15/-15]_{4s}$	2790.9	2813.8	2806.3
$[30/-30]_{4s}$	2190.6	2201.1	2186.8
$[45/-45]_{4s}$	1558.9	1562.4	1548.0
$[60/-60]_{4s}$	1239.4	1241.5	1229.6
$[75/-75]_{4s}$	1132.2	1134.5	1128.6

TABLE 2 Natural frequencies (Hz) of a cantilever mono-symmetric composite I-beam with symmetric angle-ply laminates $[\pm\theta]_{4s}$ in the flanges and web under constant axial forces at the centroid (( ): natural frequency with an axial compressive force, [ ]: natural frequency with an axial tensile force).

Mode	Stacking sequences and axial force											
	$[0]_{16}$		$[15/-15]_{4s}$		$[30/-30]_{4s}$		$[45/-45]_{4s}$		$[60/-60]_{4s}$		$[75/-75]_{4s}$	
	P=1499.05 N		P=1406.90 N		P=1100.55 N		P=781.20 N		P=620.75 N		P=567.25 N	
	Ref. [26]	Present	Ref. [26]	Present	Ref. [26]	Present	Ref. [26]	Present	Ref. [26]	Present	Ref. [26]	Present
1	(19.087)	(19.090)	(18.505)	(18.460)	(16.401)	(16.295)	(13.841)	(13.710)	(12.342)	(12.220)	(11.791)	(11.729)
	26.295	26.298	25.508	25.478	22.641	22.561	19.130	19.024	17.063	16.963	16.294	16.244
	[31.498]	[31.501]	[30.568]	[30.542]	[27.162]	[27.087]	[22.970]	[22.866]	[20.492]	[20.393]	[19.561]	[19.512]
2	(43.267)	(43.267	(44.524)	(44.388)	(46.335)	(45.155)	(40.135)	(40.178)	(35.692)	(35.730)	(34.273)	(34.310)
	46.472	46.470	47.346	47.222	48.325	47.210	42.243	42.287	37.575	37.615	36.066	36.104
	[49.414]	[49.412]	[49.969]	[49.853]	[50.213]	[49.154]	[44.224]	[44.269]	[39.345]	[39.385]	[37.751]	[37.790]
3	(59.242)	(59.304)	(56.205)	(56.265)	(48.304)	(48.355)	(45.879)	(42.790)	(42.648)	(39.156)	(37.990)	(36.481)
	61.988	62.052	58.920	58.982	50.772	50.825	47.267	44.287	43.831	40.451	39.210	37.756
	[64.586]	[64.653]	[61.484]	[61.547]	[53.096]	[53.150]	[48.593]	[45.715]	[44.963]	[41.688]	[40.374]	[38.973]
4	(129.73)	(129.809	(127.28)	(127.084)	(118.02)	(116.806)	(104.11)	(101.808)	(93.778)	(91.419)	(88.027)	(86.926)
	138.17	138.251	135.30	135.126	124.68	123.563	109.44	107.273	98.472	96.250	92.605	91.573
	[146.02]	[146.105]	[142.77]	[142.619]	[130.94]	[129.897]	[114.47]	[112.423]	[102.92]	[100.808]	[96.927]	[95.954]

TABLE 3 Effect of eccentricity on critical bucking loads (N) of a simply supported composite I-beam with symmetric angle-ply laminates $[\pm\theta]_{4s}$ in the flanges and web.

Lay-ups	$e = 0$	$e = h/4$			$e = h/2$
		Kim et al.[32]		Present	
		ABAQUS	No shear		
$[0]_{16}$	920.8			890.3	818.6
$[15/-15]_{4s}$	832.0	809.2	810.7	810.5	757.5
$[30/-30]_{4s}$	617.8	608.1	608.7	608.0	582.2
$[45/-45]_{4s}$	427.6	423.5	423.7	422.9	410.0
$[60/-60]_{4s}$	338.4	335.5	335.6	334.9	325.3
$[75/-75]_{4s}$	311.7	308.6	308.6	308.3	298.8

TABLE 4 Effect of axial force on the critical buckling moments $\overline{M}_{cr}(\times 10^{-2})$ of a simply supported composite beam with respect to the fiber angle change in the flanges and web.

Fiber	Buckling	$\overline{P} = 0.5\overline{P}_{cr}$ (compression)		$\overline{P}$=0 (no axial force)		$\overline{P} = -0.5\overline{P}_{cr}$ (tension)	
angle	loads ($\overline{P}_{cr}$)	Present	Orthotropy	Present	Orthotropy	Present	Orthotropy
0	5.153	4.451	4.451	7.370	7.370	10.175	10.175
15	4.026	4.348	4.851	6.842	7.486	9.151	9.875
30	1.404	2.358	2.733	3.496	4.004	4.472	5.068
45	0.454	1.105	1.192	1.599	1.720	2.003	2.147
60	0.255	0.701	0.713	1.009	1.026	1.258	1.278
75	0.213	0.564	0.565	0.813	0.814	1.014	1.016
90	0.206	0.528	0.528	0.763	0.763	0.953	0.953

TABLE 5 Effect of axial force and bending moment on the first four natural frequencies of a simply supported composite beam with respect to the fiber angle change in the flanges and web.

Fiber	Axial force	Present				Orthotropy			
angle	& moment	ω_1	ω_2	ω_3	ω_4	ω_{ya_1}	ω_{yb_1}	ω_{ya_2}	ω_{xx_1}
0		2.914	6.204	18.657	19.830	2.914	6.204	18.657	19.830
30	$\overline{P} = 0.5\overline{P}_{cr}$	1.591	6.010	9.655	10.225	1.667	6.936	9.732	10.352
60	$\overline{M} = 0.5\overline{M}_{cr}$	0.684	4.128	4.158	4.408	0.688	4.231	4.132	4.415
90		0.614	3.493	3.710	3.966	0.614	3.493	3.710	3.966
0		3.980	7.522	19.654	20.148	3.980	7.522	19.654	20.148
30	$\overline{P} = 0$	2.224	6.377	10.069	10.521	2.335	7.237	10.290	10.518
60	$\overline{M} = 0.5\overline{M}_{cr}$	0.963	4.254	4.345	4.486	0.969	4.324	4.357	4.486
90		0.864	3.584	3.911	4.030	0.864	3.584	3.911	4.030
0		4.769	8.666	20.461	20.518	4.769	8.666	20.518	20.461
30	$\overline{P} = -0.5\overline{P}_{cr}$	2.694	6.732	10.353	10.899	2.832	7.532	10.802	10.681
60	$\overline{M} = 0.5\overline{M}_{cr}$	1.175	4.348	4.515	4.595	1.182	4.415	4.568	4.555
90		1.053	3.675	4.092	4.098	1.053	3.675	4.098	4.092

TABLE 6 Effect of axial force on the critical buckling moments $\overline{M}_{cr}(\times 10^{-2})$ of a simply supported composite beam with respect to the fiber angle change in the bottom flange.

Fiber	Buckling	$\overline{P} = 0.5\overline{P}_{cr}$ (compression)		$\overline{P}$=0 (no axial force)		$\overline{P} = -0.5\overline{P}_{cr}$ (tension)	
angle	loads ($\overline{P}_{cr}$)	Present	Orthotropy	Present	Orthotropy	Present	Orthotropy
0	5.153	4.451	4.451	7.370	7.370	10.175	10.175
15	4.565	4.042	4.366	6.883	7.054	9.233	9.604
30	2.771	2.498	3.201	4.895	5.007	6.071	6.789
45	1.631	1.819	2.388	3.597	3.614	4.265	4.831
60	1.259	1.621	2.087	3.117	3.119	3.655	4.121
75	1.140	1.553	1.982	2.948	2.948	3.448	3.877
90	1.112	1.536	1.955	2.905	2.905	3.397	3.815

TABLE 7 Effect of axial force and bending moment on the first four natural frequencies of a simply supported composite beam with respect to the fiber angle change in the bottom flange.

Fiber	Axial force	Present				Orthotropy			
angle	& moment	ω_1	ω_2	ω_3	ω_4	ω_{ya_1}	ω_{yb_1}	ω_{ya_2}	ω_{xx_1}
0		2.914	6.204	18.657	19.830	2.914	6.204	18.657	19.830
30	$\overline{P} = 0.5\overline{P}_{cr}$	3.049	4.108	12.652	16.205	2.629	4.355	13.595	16.240
60	$\overline{M} = 0.5\overline{M}_{cr}$	2.050	3.655	5.990	12.317	1.836	3.353	6.019	14.596
90		1.895	3.674	5.450	11.146	1.695	3.360	5.453	14.523
0		3.980	7.522	19.654	20.148	3.980	7.522	19.654	20.148
30	$\overline{P} = 0$	3.672	4.772	14.120	16.429	3.102	5.471	14.034	16.449
60	$\overline{M} = 0.5\overline{M}_{cr}$	2.650	3.712	7.014	13.492	2.148	4.027	6.850	14.703
90		2.448	3.721	6.422	12.270	2.021	3.945	6.268	14.617
0		4.769	8.666	20.461	20.518	4.769	8.666	20.518	20.461
30	$\overline{P} = -0.5\overline{P}_{cr}$	4.165	5.551	15.214	16.677	3.781	6.240	14.697	16.656
60	$\overline{M} = 0.5\overline{M}_{cr}$	3.068	4.066	7.855	14.513	2.639	4.481	7.647	14.808
90		2.857	4.022	7.226	13.254	2.487	4.353	7.040	14.710

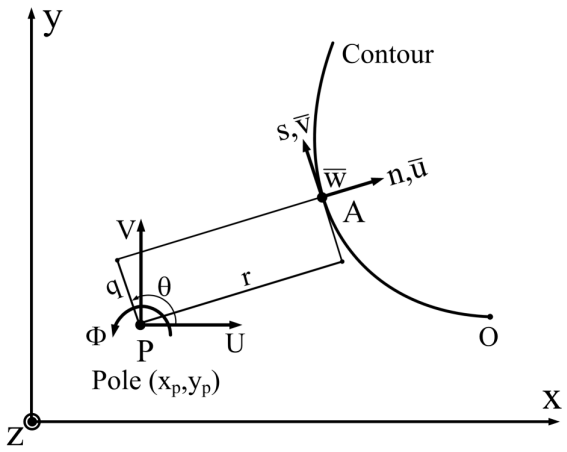

FIG. 1 Definition of coordinates in thin-walled open-section composite beams.

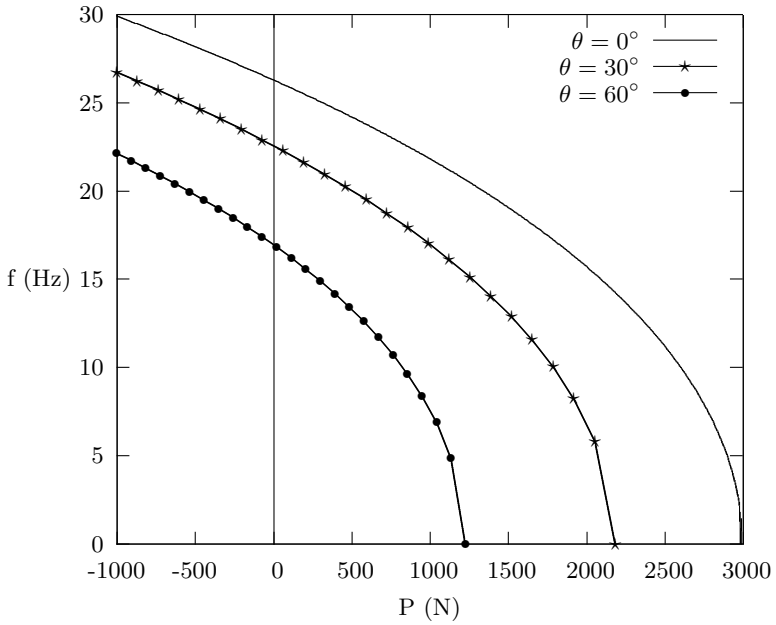

FIG. 2 Effect of axial force on the fundamental natural frequency with the fiber angles 0°, 30° and 60° in the flanges and web of a cantilever mono-symmetric composite I-beam.

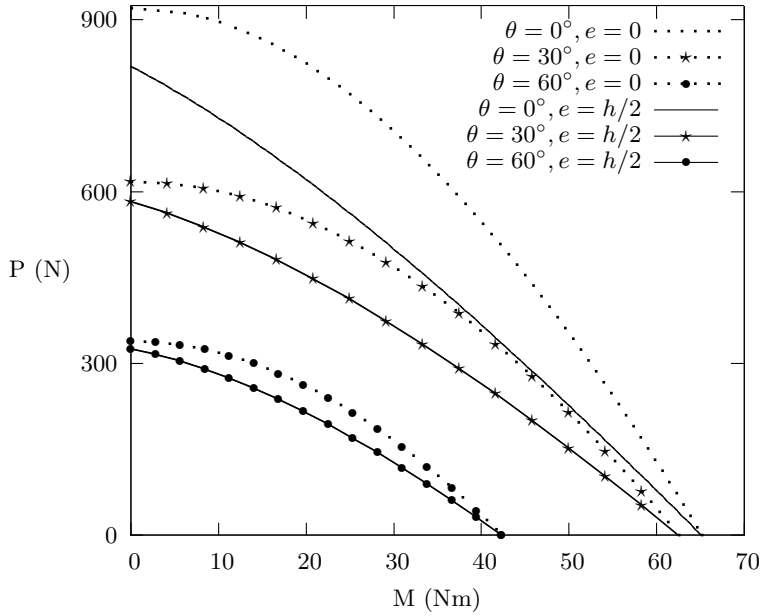

FIG. 3 Effect of eccentricity and axial compressive force on the critical buckling moments with the fiber angles 0°, 30° and 60° in the flanges and web of a simply supported composite beam.

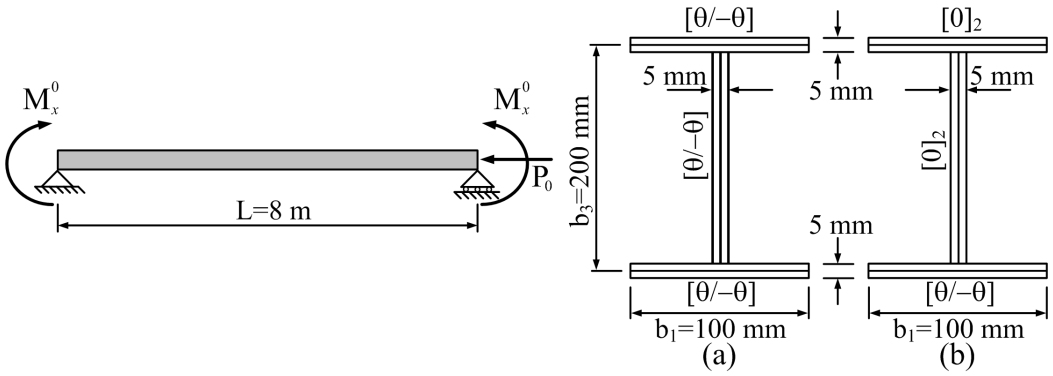

FIG. 4 Geometry and stacking sequences of a simply supported I-beam under axial load and uniform bending.

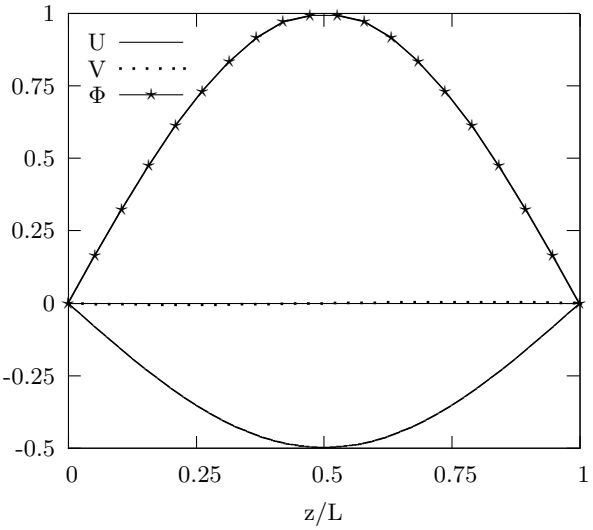

(a) Mode 1

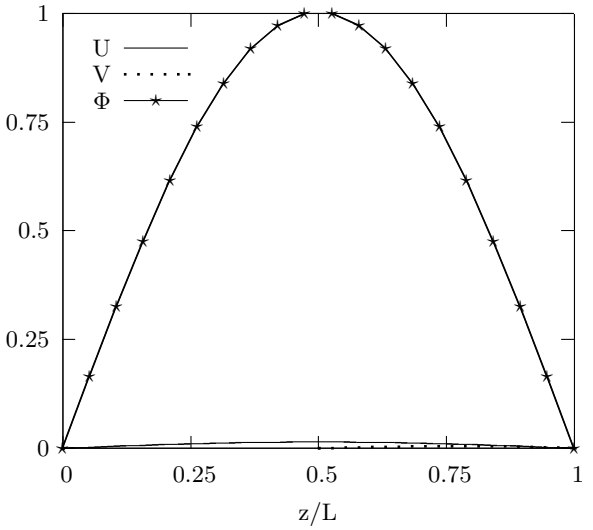

(b) Mode 2

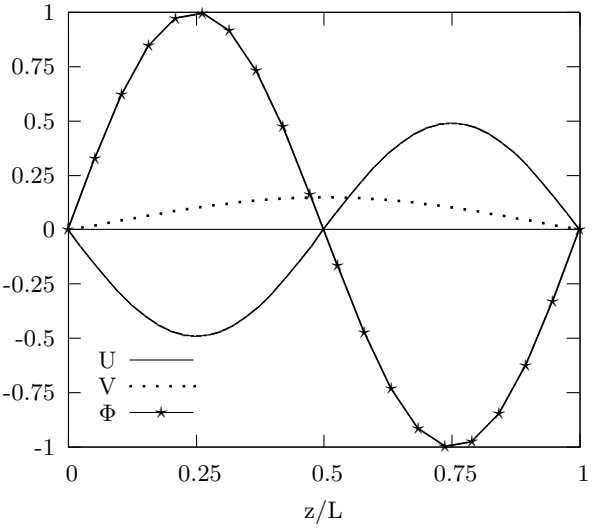

(c) Mode 3

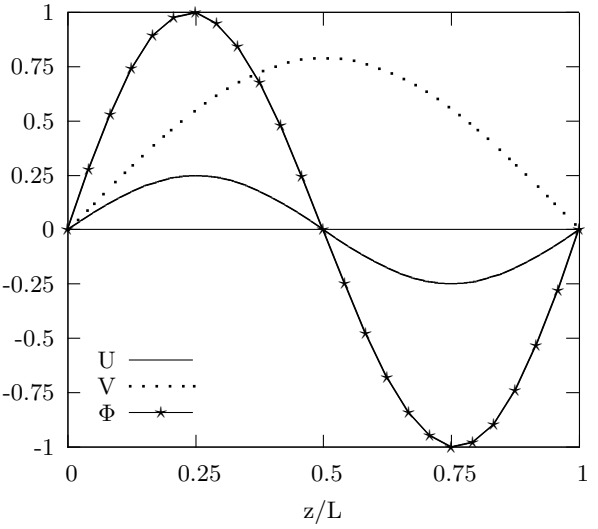

(d) Mode 4

FIG. 5 The first four normal mode shapes of the flexural and torsional components with the fiber angle 30° in the flanges and web of a simply supported composite beam under an axial compressive force ($\overline{P} = 0.5\overline{P}_{cr}$) and bending moment ($\overline{M} = 0.5\overline{M}_{cr}$).

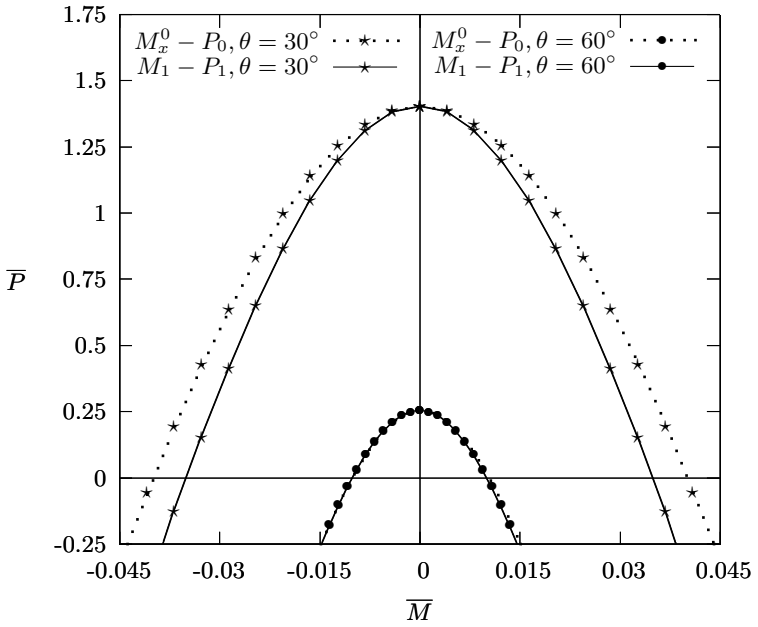

FIG. 6 Effect of axial force on the critical buckling moments with the fiber angles 30° and 60° in the flanges and web of a simply supported composite beam.

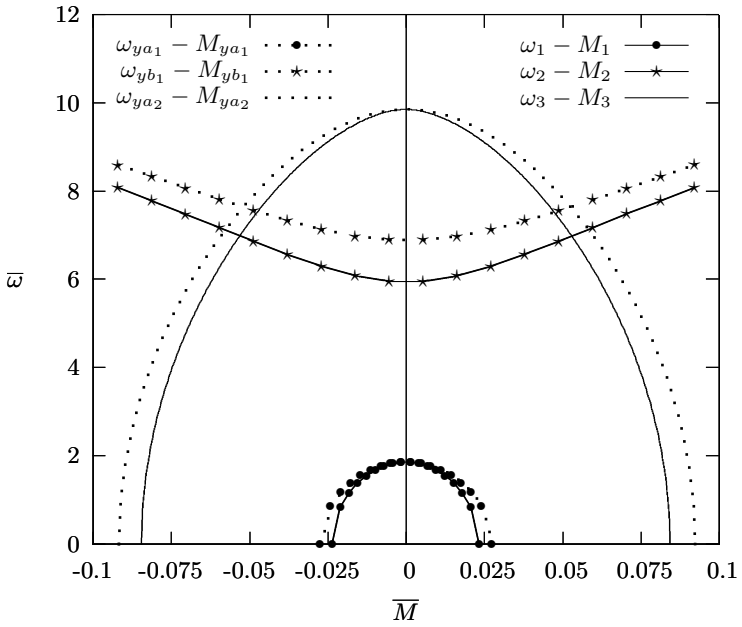

FIG. 7 Effect of bending moment on the first three natural frequencies with the fiber angle 30° in the bottom flange of a simply supported composite beam under an axial compressive force ($\overline{P} = 0.5\overline{P}_{cr}$).

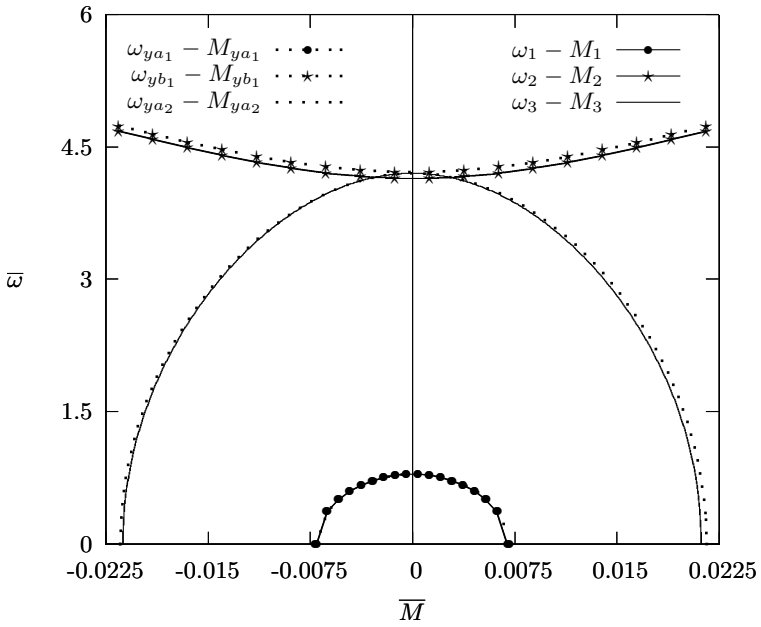

FIG. 8 Effect of bending moment on the first three natural frequencies with the fiber angle 60° in the bottom flange of a simply supported composite beam under an axial compressive force ($\overline{P} = 0.5\overline{P}_{cr}$).

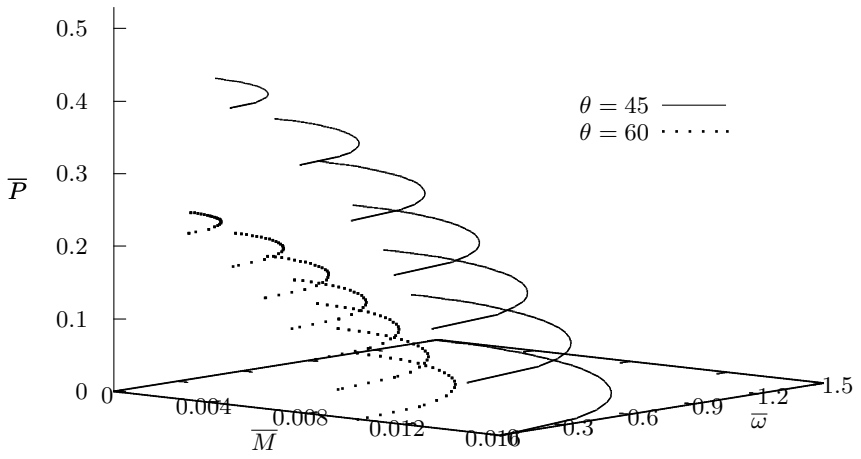

FIG. 9 Three dimensional interaction diagram of the fundamental natural frequency, bending moment and axial compressive force with the fiber angle 45° and 60° in the flanges and web of a simply supported composite beam.

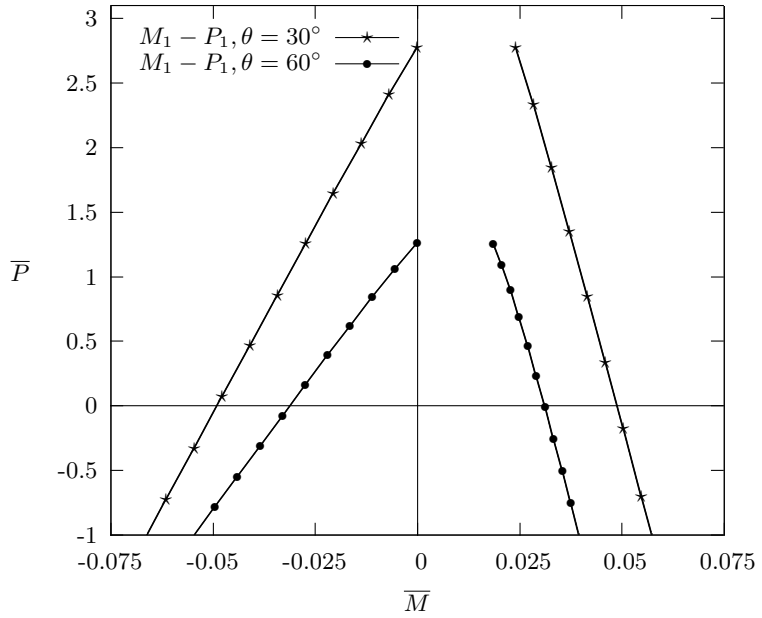

FIG. 10 Effect of axial force on the critical buckling moments with the fiber angles 30° and 60° in the bottom flange of a simply supported composite beam.

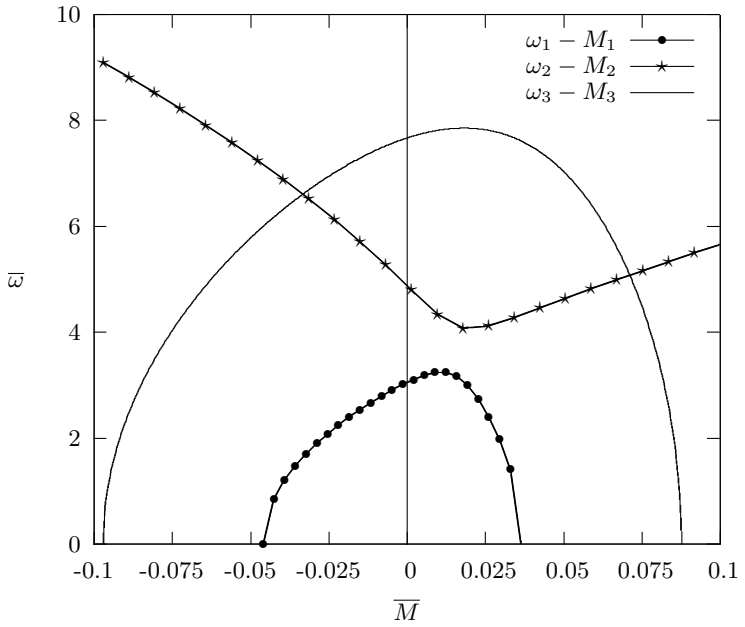

FIG. 11 Effect of bending moment on the first three natural frequencies with the fiber angle 60° in the bottom flange of a simply supported composite beam under an axial tensile force ($\overline{P} = -0.5\overline{P}_{cr}$).

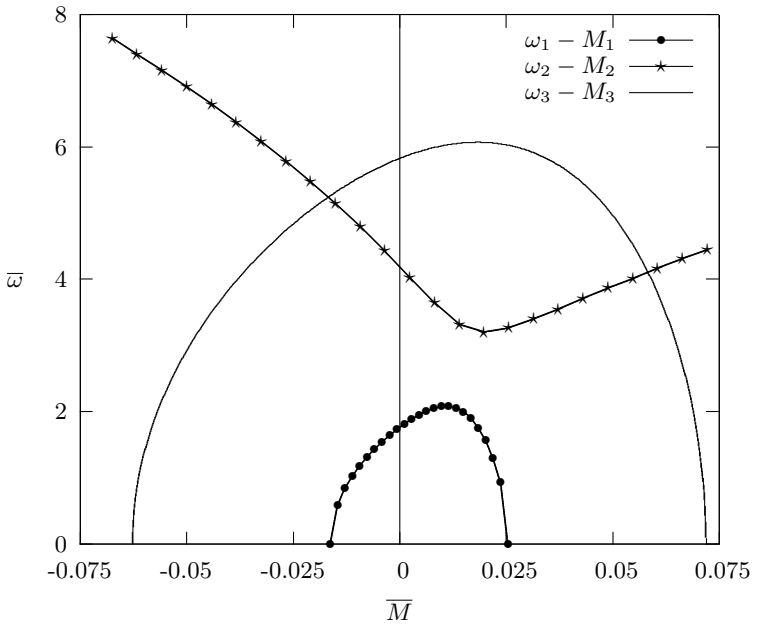

FIG. 12 Effect of bending moment on the first three natural frequencies with the fiber angle 60° in the bottom flange of a simply supported composite beam under an axial compressive force ($\overline{P} = 0.5\overline{P}_{cr}$).